Homogeneous amorphous Fe_xGe_{1-x} magnetic semiconductor films with high Curie temperature and high magnetization

Yu-feng Qin,[1] Shi-shen Yan,[1,*] Shi-shou Kang,[1] Shu-qin Xiao,[1] Qiong Zhang,[1] Xin-xin Yao,[1] Tong-shuai Xu,[1] Yu-feng Tian,[1] You-yong Dai,[1] Guo-lei Liu,[1] Yan-xue Chen,[1] Liang-mo Mei,[1] Gang Ji,[2] and Ze Zhang[3]

[1]*School of Physics and National Key Laboratory of Crystal Materials, Shandong University, Jinan, Shandong 250100, P. R. China*

[2]*Institute of Biophysics, Chinese Academy of Sciences, Beijing 100101, P. R. China*

[3]*Institute of Microstructure and Property of Advanced Materials, Beijing University of Technology, Beijing 100124, P. R. China*

(Received 27 November 2010; revised manuscript received 22 April 2011; published 30 June 2011)

Homogeneous amorphous Fe_xGe_{1-x} ($0.3 \leqslant x \leqslant 0.5$) FMS films with a high Fe concentration were synthesized under thermal nonequilibrium condition by magnetron cosputtering. The microstructure, magnetism, electrical transport, and ferromagnetic resonance were systematically studied. The results indicate that Fe_xGe_{1-x} films have intrinsic ferromagnetism with a high Curie temperature and magnetization. The saturation magnetization can be well fitted by Bloch's spin-wave formula in a wide temperature range. Quantitative analysis of electrical transport reveals that Fe_xGe_{1-x} FMS films show conductivity of weakly localized carriers (holes) on the metallic side. Moreover, the anomalous Hall resistivity is proportional to the magnetization for all samples, indicating the carriers are spin polarized and the ferromagnetism is intrinsic. The ferromagnetic resonance further reveals that the $Fe_{0.5}Ge_{0.5}$ thin films have uniform collective ferromagnetism. Therefore, Fe_xGe_{1-x} ferromagnetic semiconductors with a high Curie temperature and magnetization have potential application in spintronic devices as a highly efficient spin injection source.

DOI: 10.1103/PhysRevB.83.235214 PACS number(s): 75.50.Pp, 75.30.Gw, 72.25.Dc

I. INTRODUCTION

In recent years, ferromagnetic semiconductors (FMSs), which simultaneously exhibit spontaneous long-ranged ferromagnetic order and semiconducting properties, have attracted a great deal of attention because of their potential applications in spintronic devices. Compared with the well-explored III-V and II-VI FMSs, such as $Ga_{1-x}Mn_xAs$[1,2] and $Zn_{1-x}Co_xO$,[3] group-IV Ge-based FMSs are more attractive for compatibility with mainstream Si-based processing technology, as well as high hole mobility. Park *et al.*[4] first reported that epitaxial single-crystal Mn_xGe_{1-x} films showed ferromagnetism and the Curie temperature increased linearly with Mn concentration from 25 K to 116 K. Shuto *et al.*[5] claimed that the epitaxial $Fe_{0.175}Ge_{0.825}$ film showed intrinsic ferromagnetism with a Curie temperature of 170 K. Amorphous Ge-based FMSs with a high Mn concentration were also reported,[6,7] with a Curie temperature of ~213 K. And for codoped $Mn_{0.13}Fe_{0.06}Ge_{0.81}$[8] and $Co_{0.12}Mn_{0.03}Ge_{0.85}$,[9] the Curie temperatures were 209 K and 270 K, respectively. Currently, the main problem lies in that the Curie temperature of most Ge-based magnetic semiconductors with intrinsic ferromagnetism is below room temperature.

On the other hand, ferromagnetism with a relative high Curie temperature may occur because of composition inhomogeneity and/or second phases in the host phase. Cho *et al.*[10,11] reported that bulk single-crystal Mn-, Cr-, or Fe-doped Ge-based materials showed ferromagnetism and the highest Curie temperature was 285 K, but the magnetic properties of the samples were clearly coherent with the presence of intermetallic compounds. Goswami *et al.*[12] claimed that Fe-rich nanomagnets (Fe_3Ge_2) were observed in an epitaxial single-crystal Ge matrix with a Curie temperature of $\leqslant$230 K. Jamet *et al.*[13] reported a high-T_C (>400 K) ferromagnetic phase of a (Ge,Mn) epitaxial layer, in which well-defined Mn-rich nanocolumns were embedded in a Mn-poor matrix. However, the ferromagnetism from the clusters or the second phases may be just local ferromagnetism, rather than the long-ranged ferromagnetism, which limits the applications of Ge-based materials in spintronic devices.

For practical applications of Ge-based FMSs, intrinsic ferromagnetism, high Curie temperature, and spin-polarized carriers are highly desirable. Theoretical calculations predicted that Ge-based semiconductors with high Fe doping were easily ferromagnetic compared with Mn doping,[14] but they were studied less often experimentally. Also, Paul and Sanyal[15] revealed that Fe doping in MnGe led to an increase in ferromagnetic interactions, as well as a decrease in the overall clustering tendency between magnetic dopants. Therefore, further systematic study on the Fe_xGe_{1-x} magnetic semiconductor with a high Fe concentration is necessary for the desirable properties.

For this paper, homogeneous amorphous Fe_xGe_{1-x} FMS films with high Fe concentrations (30–50 at.%) were synthesized under a thermal nonequilibrium condition by magnetron cosputtering technology. A high Curie temperature >350 K and a high saturation magnetization of 27.8 emu/g at 300 K were obtained in $Fe_{0.4}Ge_{0.6}$ films. The conductivity is on the metallic side of the metal-insulator transition. In addition, we found that the anomalous Hall resistivity is proportional to the magnetization, indicating the carriers are spin polarized and the ferromagnetism is intrinsic. Finally, uniform collective ferromagnetism was confirmed by ferromagnetic resonance.

II. EXPERIMENTAL DETAILS

Fe_xGe_{1-x} films were synthesized on glass substrates by magnetron cosputtering equipment with Fe (99.99%) and Ge (99.99%) targets. The thickness of all films was 300 nm. The base pressure of the chamber was better than 3.0×10^{-5} Pa, and the pressure of pure Ar (99.99%) was kept at 1.4 Pa

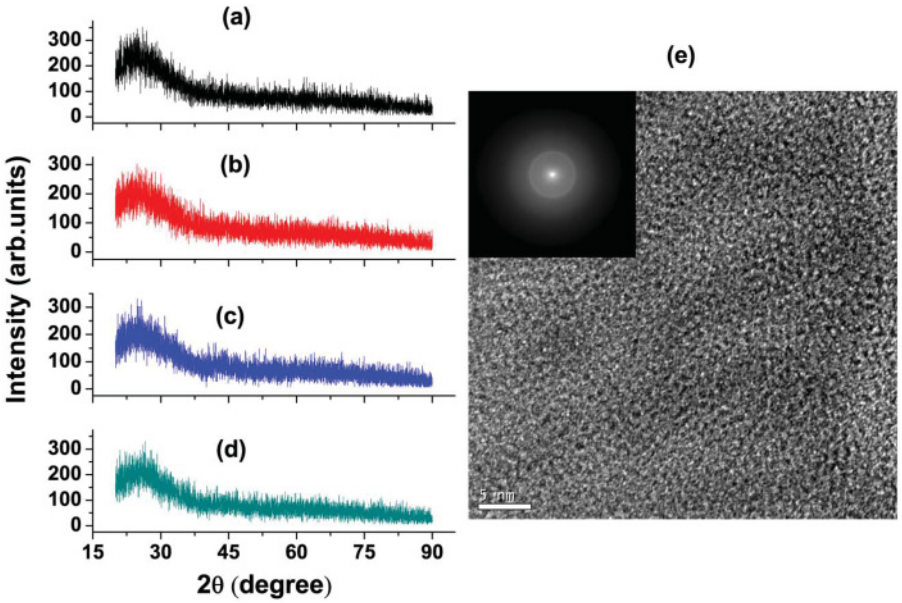

FIG. 1. (Color online) (a) The XRD patterns of the glass substrate. (b)–(d) The XRD patterns of the Fe_xGe_{1-x} films, with Fe concentrations of 50%, 40%, and 30%, respectively. (e) A high-resolution TEM image of the $Fe_{0.4}Ge_{0.60}$ film observed in the cross-section view. The scale bar is 5 nm. The inset of (e) is a selected-area electron diffraction pattern of the $Fe_{0.4}Ge_{0.6}$ film.

during sputtering. The growth rate of Fe was fixed at 0.2 Å/s, whereas the growth rate of Ge varied from 0.38 to 0.89 Å/s. In this way, the concentration of Fe in Fe_xGe_{1-x} films can be tuned from 30 to 50 at.%. During sputtering, the substrate was rotated to ensure uniformity of the films. The glass substrate temperature was fixed at 20 °C by water cooling, which is a thermal nonequilibrium growth condition for Fe_xGe_{1-x} films. The low growth temperature on the amorphous glass substrate is important to form the amorphous Fe_xGe_{1-x} phase, which greatly enhances the solubility of Fe in Ge without impurity phases.

X-ray diffraction (XRD) with a Cu K_α radiation was used to detect the crystal structure of the films. The XRD spectra were measured as $2\theta = 20°$–$90°$, with a step size of 0.02°. A high-resolution transmission electron microscope (TEM) equipped with energy dispersive x-ray spectroscopy (EDS) and selected-area electron diffraction was used to confirm the morphology and microstructure of the films. The composition of the films was confirmed by EDS measurements. The magnetic properties were measured by a superconducting quantum interference device. We subtracted the contribution of the substrate, which was measured after etching away the films with an acid solution. Electrical transport properties, such as conductivity and Hall resistivity, were measured in a Van der Pauw configuration by a physical properties measurement system.

III. RESULTS AND DISCUSSION

A. Structure and morphology

Figures 1(a)–1(d) show the XRD patterns of the glass substrate and the Fe_xGe_{1-x} films. No XRD diffraction peaks were observed for all films with different Fe concentrations, except for the signals of amorphous glass substrate with 2θ around 25°, which indicates that the as-made films are amorphous or nanocrystal. Figure 1(e) is the high-resolution TEM image of the $Fe_{0.4}Ge_{0.6}$ film observed in the cross-section view, which evidently shows that the film is in an amorphous state and the distribution of Fe atoms is uniform in a nanoscale regime. Although the concentration of Fe was high up to 40 at.%, no pure Fe metal clusters or well-known Fe-Ge crystal phases were observed, which is in agreement with the results of XRD. The visible dark and bright stripes resulted from the local strain, which were also observed in other experiments.[16] The amorphous structure of the $Fe_{0.4}Ge_{0.6}$ film was confirmed by the wide diffraction ring of the selected-area electron diffraction, as shown in the inset of Fig. 1(e). To detect the local composition of the cross section of samples, we used a small electron beam ~2 nm in diameter for EDS measurements. Taking $Fe_{0.4}Ge_{0.6}$ thin films as an example, the measured concentration of Fe in different regions is nearly equivalent, and the average concentration is 40.3 and 59.7 at.% for Fe and Ge, respectively. Combining the XRD and TEM results, we believe that the homogeneous amorphous Fe_xGe_{1-x} films were obtained without any detectable impurity clusters or second phases.

B. Magnetic properties

Figures 2(a) and 2(b) show typical hysteresis loops of the $Fe_{0.5}Ge_{0.5}$ and $Fe_{0.4}Ge_{0.6}$, respectively, films measured at 30 K, 150 K, and 300 K with the applied magnetic field in the film plane. The ferromagnetism can be clearly seen from the development of coercivity and remanent magnetization in the hysteresis loops. The coercivity of the $Fe_{0.4}Ge_{0.6}$ film is 7 and 47 Oe at 300 K and 30 K, respectively. The saturation magnetization reaches 1.7 μ_B/Fe for $Fe_{0.5}Ge_{0.5}$ and 1.22 μ_B/Fe for $Fe_{0.4}Ge_{0.6}$ at 30 K. It is well known that there are two equilibrium phases on the Fe-Ge phase diagram in this concentration range (Fe of 30–50 at.%), i.e., $FeGe_2$ and FeGe. The former is antiferromagnetic alloy, and the latter is paramagnetic alloy, so the amorphous Fe_xGe_{1-x} FMS is not related to the $FeGe_2$ and FeGe equilibrium phases.

Figures 2(c) and 2(d) further show the anisotropic hysteresis loops of the $Fe_{0.5}Ge_{0.5}$ and $Fe_{0.4}Ge_{0.6}$ films, respectively, measured at 30 K, with the magnetic field parallel and perpendicular to the film plane. For the magnetic field perpendicular

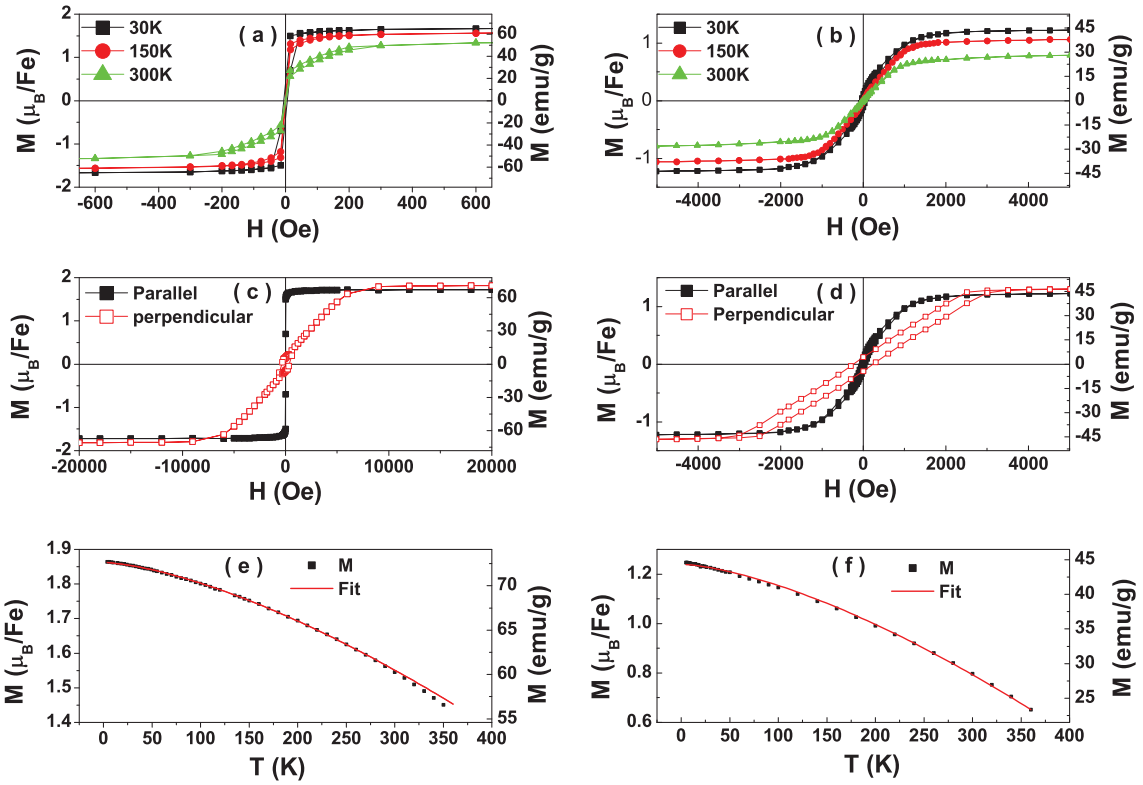

FIG. 2. (Color online) (a), (b) Hysteresis loops of the $Fe_{0.5}Ge_{0.5}$ and $Fe_{0.4}Ge_{0.6}$ films, respectively, which are measured with the applied magnetic field parallel to the film plane at temperatures of 30 K, 150 K, and 300 K. (c), (d) Anisotropic hysteresis loops measured with the applied magnetic field parallel and perpendicular to the film plane at 30 K for $Fe_{0.5}Ge_{0.5}$ and $Fe_{0.4}Ge_{0.6}$ films, respectively. (e), (f) Temperature dependence of saturation magnetization measured with a 10 000 Oe magnetic field parallel to the film plane of $Fe_{0.5}Ge_{0.5}$ and $Fe_{0.4}Ge_{0.6}$ films, respectively. The solid lines of (e) and (f) show the fitting by Eq. (1), with $M_0 = 1.86\,\mu_B$/Fe, $a = 3.2 \times 10^{-5}\mathrm{K}^{-3/2}$, for the $Fe_{0.5}Ge_{0.5}$ film and $M_0 = 1.24\,\mu_B$/Fe, $a = 6.9 \times 10^{-5}\mathrm{K}^{-3/2}$, for the $Fe_{0.4}Ge_{0.6}$ film.

to the film plane, the magnetization is hard to saturate because of the demagnetization field of thin films. The $Fe_{0.5}Ge_{0.5}$ film shows a high saturation field (the demagnetization field), because of high magnetization, as compared with the $Fe_{0.4}Ge_{0.6}$ film. On the other hand, the hysteresis loops in the film plane are easy to saturate, which shows the soft magnetic property with the easy magnetization plane. The obvious demagnetization anisotropy implies that the thin film forms a continuous magnetic layer rather than a magnetic granular film or magnetic clusters embedded in the Ge matrix. However, there is no in-plane anisotropy for all samples with different Fe compositions, which is consistent with the homogeneous amorphous state of Fe_xGe_{1-x} films. Although the magnetic anisotropy was observed in other FMSs,[1] it was not reported in Ge-based FMSs.

Figures 2(e) and 2(f) show the temperature dependence of the saturation magnetization of the $Fe_{0.5}Ge_{0.5}$ and $Fe_{0.4}Ge_{0.6}$ films, respectively, which was measured with a 10 000 Oe magnetic field in the film plane from 5 K to 350 K. For the $Fe_{0.5}Ge_{0.5}$ film, the saturation magnetization decreases monotonously from 1.85 to 1.45 μ_B/Fe with increasing temperature. For the $Fe_{0.4}Ge_{0.6}$ film, it monotonously changes from 1.23 to 0.65 μ_B/Fe. As shown in Figs. 2(e) and 2(f), both *M-T* curves can be well fitted by Bloch's spin-wave formula, which indicates the long-ranged ferromagnetic interaction between the Fe ions mediated by the hole carriers.[17] Such fitting is another character of good FMSs.[18,19] The Bloch spin-wave formula used for fitting can be written as following

$$M(T) = M_0(1 - aT^{3/2}), \tag{1}$$

where M_0 is the saturation magnetization at 0K and a is the Bloch constant. The experimental *M-T* curves are in good agreement with Eq. (1) in the wide temperature range from 5 K to 250 K for the $Fe_{0.5}Ge_{0.5}$ film and in the whole temperature range for the $Fe_{0.4}Ge_{0.6}$ film. From the experimental *M-T* curves, we see that the Curie temperature is >350 K for these films. The fitting M_0 is 1.86 μ_B/Fe for the $Fe_{0.5}Ge_{0.5}$ film and 1.24 μ_B/Fe for the $Fe_{0.4}Ge_{0.6}$ film. On the other hand, the Bloch constant a was found to decrease with increasing Fe concentration, from $6.9 \times 10^{-5}\mathrm{K}^{-3/2}$ for the $Fe_{0.4}Ge_{0.6}$ film to $3.2 \times 10^{-5}\mathrm{K}^{-3/2}$ for the $Fe_{0.5}Ge_{0.5}$ film, which is different from the behavior of ferromagnetic nanoparticles.[20] This means that the spontaneous magnetization decreases more quickly with increasing temperature for low Fe concentration samples, because only the high concentration of Fe atoms can provide sufficient ferromagnetic ions and carriers to establish a robust carrier-mediated long-ranged ferromagnetism.

Figure 3 shows the zero field cooling (ZFC) and field cooling (FC) magnetization of the $Fe_{0.4}Ge_{0.6}$ film as a function of temperature, with a measuring field of 50 Oe perpendicular to the film plane. After cooling the sample in the zero magnetic field from 380 K to 4 K, the ZFC curve was

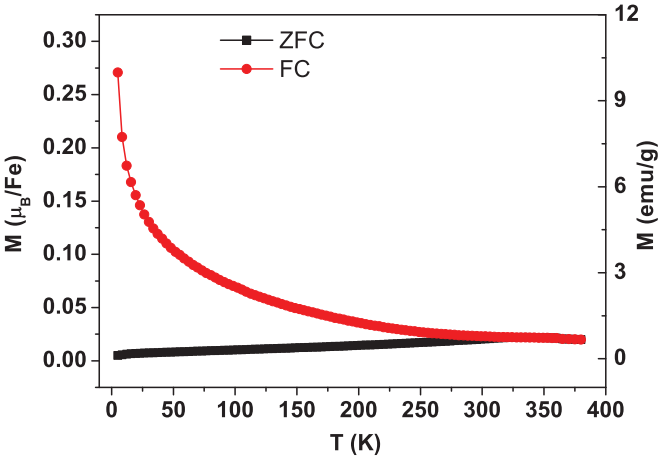

FIG. 3. (Color online) The temperature dependence of ZFC and FC magnetization of the $Fe_{0.4}Ge_{0.6}$ film. The external magnetic field of 50 Oe was perpendicular to the film plane during the measurements. The ZFC and FC curves overlap above 330 K.

measured from 4 K to 380 K. As for the FC measurement, the sample was first cooled from 380 K to 4 K with a 20 000-Oe magnetic field perpendicular to the film plane, and then the FC curve was obtained in a similar procedure. The ZFC and FC curves begin to overlap above 330 K, a temperature much lower than the Curie temperature of the $Fe_{0.4}Ge_{0.6}$ film. There is no peak in the ZFC curve below room temperature, which is different from the behavior of small ferromagnetic particles.[12,21] Supposing that the cross point of ZFC and FC curves is at the blocking temperature of isolated superparamagnetic particles and the magnetic anisotropic field $H_K = 2500$ Oe in Fig. 2(d) is adopted, the particles' diameter should be ~42 nm, which should have been observed in XRD patterns and high-resolution TEM images. Therefore, all magnetic measurements should show uniform collective ferromagnetism, which is consistent with the homogenous Fe_xGe_{1-x} films.

C. Electrical transport properties

Figure 4 shows the temperature dependence of the conductivity σ_{xx} for different Fe_xGe_{1-x} films. Despite the high concentration of Fe, the conductivity σ_{xx} smoothly decreases with the temperature, which is a typical feature of semiconductor conduction. The conductivity changes little in the whole measured temperature range for all films, indicating that the carriers are weakly localized. In doped amorphous semiconductors, on the metallic side of the metal-insulator transition,[22,23] the σ_{xx}-T relation can be written by

$$\sigma_{xx} = \sigma_0 + c_1 T^{1/2} + c_2 T, \tag{2}$$

where σ_0 is the conductivity at $T = 0$ K, $c_1 T^{1/2}$ arises from the Coulomb interaction of carriers in the disordered materials, and $c_2 T$ originates from the inelastic electron-phonon scattering of weakly localized carriers. As illustrated in Fig. 4, the experimental σ_{xx}-T curves are well fitted by Eq. (2) in the low temperature range, indicating electrical transport behavior on the metallic side of the metal-insulator transition. Comparing Figs. 4(a)–4(c), it can be found that

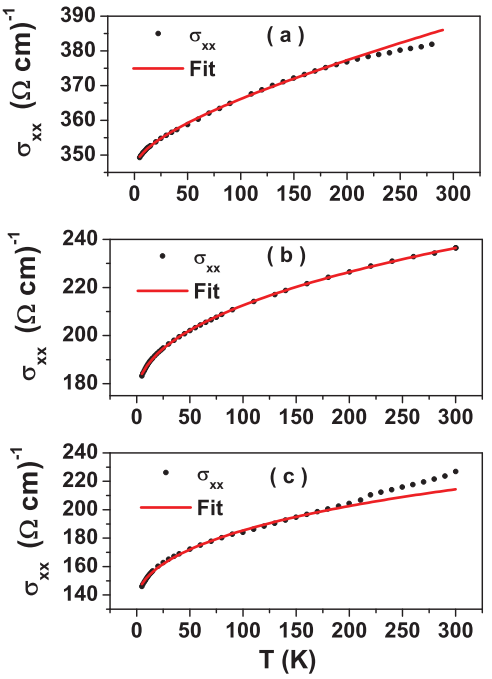

FIG. 4. (Color online) The temperature dependence of conductivity σ_{xx} for different compositional films. The solid lines show the fitting by Eq. (2). (a) For the $Fe_{0.5}Ge_{0.5}$ film, the fitting is good from 5 K to 200 K, with $\sigma_0 = 346\ \Omega^{-1}\,\mathrm{cm}^{-1}$, $c_1 = 1.57\ \Omega^{-1}\,\mathrm{cm}^{-1}\mathrm{K}^{-1/2}$, and $c_2 = 0.047\ \Omega^{-1}\,\mathrm{cm}^{-1}\mathrm{K}^{-1}$. (b) For the $Fe_{0.4}Ge_{0.6}$ film, the fitting is good from 5 K to 300 K, with $\sigma_0 = 175\ \Omega^{-1}\,\mathrm{cm}^{-1}$, $c_1 = 4.00\ \Omega^{-1}\,\mathrm{cm}^{-1}\mathrm{K}^{-1/2}$, and $c_2 = -0.03\ \Omega^{-1}\,\mathrm{cm}^{-1}\mathrm{K}^{-1}$. (c) For the $Fe_{0.3}Ge_{0.7}$ film, the fitting is good from 5 K to 200 K, with $\sigma_0 = 135\ \Omega^{-1}\,\mathrm{cm}^{-1}$, $c_1 = 5.62\ \Omega^{-1}\,\mathrm{cm}^{-1}\mathrm{K}^{-1/2}$, and $c_2 = -0.06\ \Omega^{-1}\,\mathrm{cm}^{-1}\mathrm{K}^{-1}$.

the conductivity decreases with the concentration of Fe for any given temperature <300 K. As the concentration of Fe decreasing, the carrier (hole) density decreases and the localization of carriers clearly dominates. In this case, it is easy to understand that the fitting parameter σ_0 decreases with the concentration of Fe, i.e., $\sigma_0 = 346\ \Omega^{-1}\,\mathrm{cm}^{-1}$ for the $Fe_{0.5}Ge_{0.5}$ film, $\sigma_0 = 175\ \Omega^{-1}\,\mathrm{cm}^{-1}$ for the $Fe_{0.4}Ge_{0.6}$ film, and $\sigma_0 = 135\ \Omega^{-1}\,\mathrm{cm}^{-1}$ for the $Fe_{0.3}Ge_{0.7}$ film. On the contrary, the conductivity from the contribution of the Coulomb interaction of carriers increases with decreasing the concentration of Fe, because the Coulomb screening effect is weaker at a lower carrier density. Therefore, the fitting parameter c_1 increases with decreasing the concentration of Fe, i.e., $c_1 = 1.57\ \Omega^{-1}\,\mathrm{cm}^{-1}\mathrm{K}^{-1/2}$ for the $Fe_{0.5}Ge_{0.5}$ film, $c_1 = 4.00\ \Omega^{-1}\,\mathrm{cm}^{-1}\mathrm{K}^{-1/2}$ for the $Fe_{0.4}Ge_{0.6}$ film, and $c_1 = 5.62\ \Omega^{-1}\,\mathrm{cm}^{-1}\mathrm{K}^{-1/2}$ for the $Fe_{0.3}Ge_{0.7}$ film. We also measured the magnetoresistance (MR) of the samples, i.e., the sheet resistivity as a function of the magnetic field. The MR is negative, and its value is very small (<0.1% in the field of 6 T) in the whole measured temperature range from 5 K to 300 K, no matter whether the applied field is parallel or perpendicular to the film plane. Usually, small negative MR is considered as a sign of moment-carrier interactions and spin-polarized carriers in strongly correlated systems,[2,22–25] in contrast to small positive MR found in ordinary nonmagnetic metals[22,23] and the large positive MR observed in disordered or

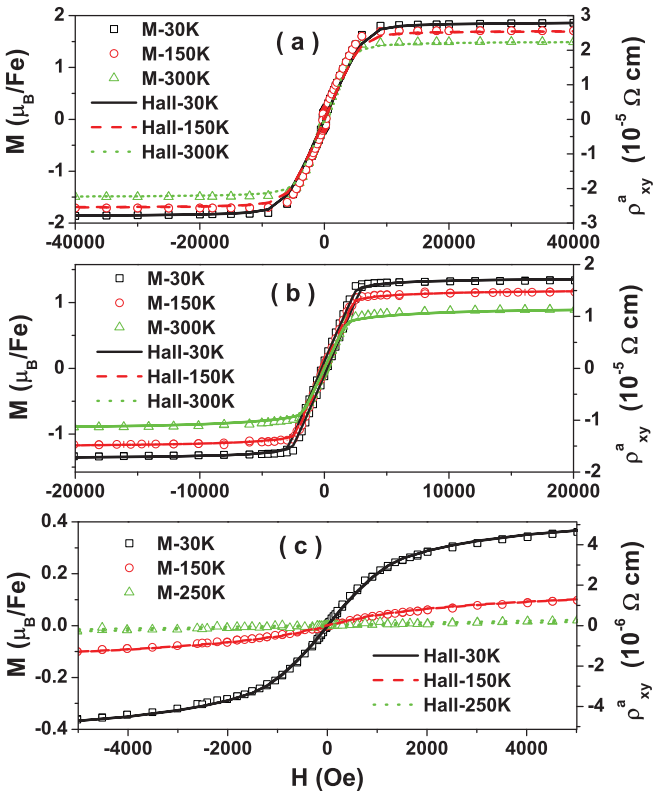

FIG. 5. (Color online) *M-H* hysteresis loops and the corresponding anomalous Hall resistivity ρ^a_{xy}-*H* loops of (a) $Fe_{0.5}Ge_{0.5}$, (b) $Fe_{0.4}Ge_{0.6}$, and (c) $Fe_{0.3}Ge_{0.7}$ films. The measuring temperature is showed. The scatters represent magnetization, and the lines represent anomalous Hall resistivity.

inhomogeneous semiconductors.[13,26] The advantage of small negative MR in the system of moment-carrier interactions is that the influence of MR on the Hall effect is negligible.

The Hall effect of the films was measured at different temperatures, and the anomalous Hall effect was dominant below the Curie temperature. The Hall resistivity is usually written by the empirical formula

$$\rho_{xy}(H,T) = R_0(T)\mu_0 H + R_S(H,T)M(H,T), \qquad (3)$$

where H is the external magnetic field, μ_0 is the vacuum permeability, and $R_0(T)$ and $R_S(H,T)$ are the ordinary and anomalous Hall coefficients at temperature T and magnetic field H, respectively. Thus, the experimental Hall resistivity can be divided into two parts: the first term in Eq. (3), representing the ordinary Hall effect $\rho^o_{xy}(H,T) = R_0(T)\mu_0 H$, which is proportional to H, and the second term in Eq. (3), representing the anomalous Hall resistivity $\rho^a_{xy}(H,T) = R_S(H,T)M(H,T)$, which is proportional to $M(H,T)$. When the external field is larger than the saturation magnetic field, the anomalous Hall resistivity will be saturated and only the ordinary Hall effect remains. In this case, the carriers (holes in *p*-type Fe_xGe_{1-x} semiconductor) density can be derived from the slope of Hall resistivity $\rho_{xy}(H)$ in a high magnetic field region from 30 000 to 60 000 Oe, where $\rho_{xy}(H)$ is proportional to the magnetic field. We obtained the concentration of hole carriers: $7.3 \times 10^{21}/\mathrm{cm}^3$ for $Fe_{0.5}Ge_{0.5}$, $5.6 \times 10^{21}/\mathrm{cm}^3$ for $Fe_{0.4}Ge_{0.6}$, and $3.4 \times 10^{21}/\mathrm{cm}^3$ for $Fe_{0.3}Ge_{0.7}$ films at 30 K. Clearly, the hole density increases with increasing Fe concentration. Such high hole density is responsible for the observed high Curie temperature of Fe_xGe_{1-x} magnetic semiconductor films.

The anomalous Hall resistivity ρ^a_{xy} as a function of the magnetic field (ρ^a_{xy}-*H* curve) for each sample at different temperatures is shown in Fig. 5. The corresponding *M-H* curves with the same magnetic field perpendicular to the film plane at the same temperature are also illustrated in this figure. With proper scaling, we can see that the ρ^a_{xy}-*H* and *M-H* curves are superimposed perfectly for each sample at a given temperature. Such perfect accordance between ρ^a_{xy}-*H* and *M-H* curves indicates that a single ferromagnetic ordering phase exists,[7,25] and the observed ferromagnetism is intrinsic. We believe that the high Fe concentration in our films provides the high concentration of holes and localized spins of Fe. Therefore, the intrinsic ferromagnetism should originate from the ferromagnetic exchange coupling between strongly localized spins of Fe 3*d* electrons, which was mediated by the weakly localized *s*, *p* holes resulting from Fe partially replacing Ge sites. The strong anomalous Hall effect with obvious hysteresis indicates that the carriers are polarized.[1,2,4,25]

The relationship between $\rho^a_{xy}(H,T)$ and $M(H,T)$ is further shown in Fig. 6 for all data in Fig. 5. We found that

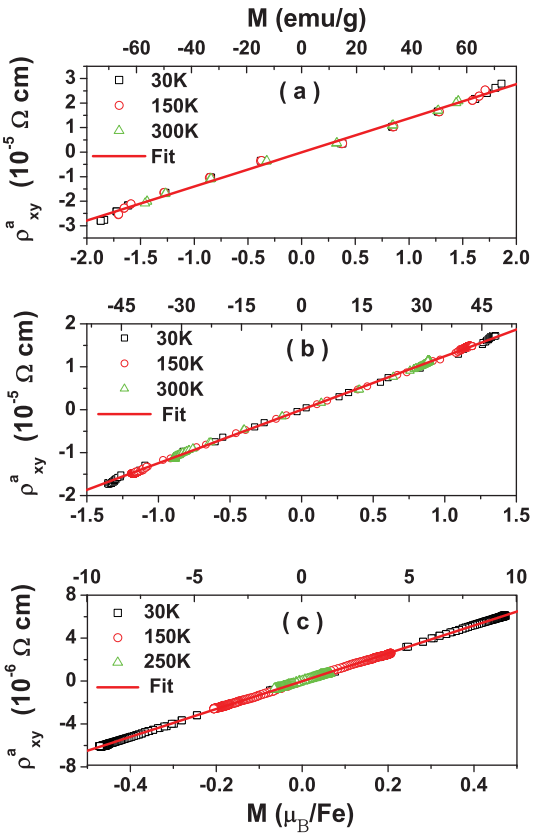

FIG. 6. (Color online) Relation between ρ^a_{xy} and M, corresponding to all data in Fig. 5, which were measured at different temperatures and magnetic fields. The solid line is the linear fitting, and the slope is the value of $R_S(H,T)$ for each sample. (a) For $Fe_{0.5}Ge_{0.5}$, $R_S(H,T) = 3.57 \times 10^{-7}\ \Omega^{-1}\,\mathrm{cm}^{-1}\mathrm{g}^{-1}\mathrm{emu}^{-1}$. (b) For $Fe_{0.4}Ge_{0.6}$, $R_S(H,T) = 3.48 \times 10^{-7}\ \Omega^{-1}\,\mathrm{cm}^{-1}\mathrm{g}^{-1}\mathrm{emu}^{-1}$. (c) For $Fe_{0.3}Ge_{0.7}$, $R_S(H,T) = 6.49 \times 10^{-7}\ \Omega^{-1}\,\mathrm{cm}^{-1}\mathrm{g}^{-1}\mathrm{emu}^{-1}$.

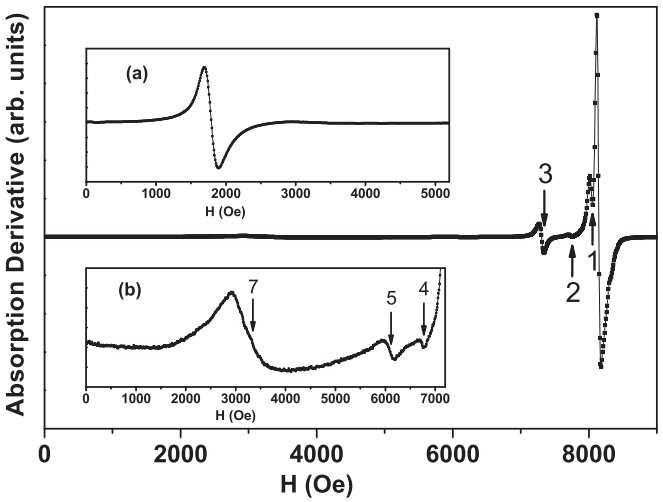

FIG. 7. The derivative spectra of ferromagnetic resonance of the $Fe_{0.5}Ge_{0.5}$ thin film measured at room temperature for the applied magnetic field perpendicular to the film plane with the frequency of 9.77 GHz. Its low magnetic field region was enlarged in inset (b). The numbers 1, 2, 3, 4, 5, and 7 mark the spin-wave modes. Inset (a) is the ferromagnetic resonance when the applied magnetic field is in the film plane.

the experimental anomalous Hall resistivity $\rho_{xy}^{a}(H,T)$ is proportional to the magnetization $M(H,T)$ for all samples at any given magnetic field and temperature below the Curie temperature. This means that for each Fe_xGe_{1-x} film, the slope, i.e., the value of $R_S(H,T)$, is a constant within the error of the experiments, which does not depend on the external magnetic field and temperature.

D. Ferromagnetic resonance

To further check the ferromagnetism and its uniformity for Fe_xGe_{1-x} magnetic semiconductor thin films, ferromagnetic resonance was done on some samples. Figure 7 shows the derivative spectra of ferromagnetic resonance of the $Fe_{0.5}Ge_{0.5}$ thin film, which was measured at room temperature with a frequency of 9.77 GHz. When the applied magnetic field was in the film plane (Fig. 7 inset (a)), only one uniform resonance peak with strong intensity and narrow width was found, which is consistent with the uniform magnetization of amorphous ferromagnetic thin film. If the second magnetic phase exists in the $Fe_{0.5}Ge_{0.5}$ thin film, an additional resonance peak should be detected. When the applied magnetic field was perpendicular to the film plane, several subsidiary peaks below the uniform resonance peak were observed, as shown in Fig. 7 and its (b) inset. In the case of perpendicular magnetic fields, the separation between the subsidiary resonance field and the uniform resonance field is ~95, 392, 844, 1408, 2078, and 4800 Oe. The ratio of separation is $\sim 1^2:2^2:3^2:4^2:5^2:7^2$. When the angle between the external field and the film normal increases, all resonance fields gradually decrease; finally, all subsidiary peaks except the uniform resonance peak disappear at an angle larger than 25°. According to the spin-wave theory of magnetic thin films,[27] the separation between the resonance field of the nth spin-wave mode and that of the uniform resonance mode is proportional to n^2. The observed n^2 law in the $Fe_{0.5}Ge_{0.5}$ thin film means that the subsidiary peaks below the uniform resonance peak are spin-wave modes. A series of spin-wave modes accompanying a strong and narrow uniform resonance mode reveals that the $Fe_{0.5}Ge_{0.5}$ thin film has uniform collective ferromagnetism.

IV. CONCLUSIONS

Homogeneous amorphous Fe_xGe_{1-x} FMS films with a high Fe concentration were synthesized. The Curie temperature is >350 K. Quantitative analysis of electrical transport reveals that Fe_xGe_{1-x} FMS films show conductivity of weakly localized carriers (holes) on the metallic side. Moreover, the anomalous Hall resistivity is proportional to the magnetization for all films, indicating the carriers are spin polarized and the ferromagnetism is intrinsic. The ferromagnetic resonance further reveals that the Fe_xGe_{1-x} thin films have uniform collective ferromagnetism. The Fe_xGe_{1-x} FMS with a high Curie temperature and magnetization may have application in spintronic devices as a highly efficient spin injection source.

ACKNOWLEDGMENTS

This work was supported by the National Basic Research Program of China Grants No. 2007CB924903 and No. 2009CB929202, Grant No. JQ200901, and National Science Foundation (NSF) Grant No. 10974120.

*shishenyan@sdu.edu.cn

[1] H. Ohno, A. Sher, F. Matsukura, A. Oiwa, A. Eudo, S. Katsumoto, and Y. Iye, Appl. Phys. Lett. **69**, 363 (1996).
[2] H. Ohno, Science **281**, 951 (1998).
[3] G. L. Liu, Q. Cao, J. X. Deng, P. F. Xing, Y. F. Tian, Y. X. Chen, S. S. Yan, and L. M. Mei, Appl. Phys. Lett. **90**, 052504 (2007).
[4] Y. D. Park, A. T. Hanbicki, S. C. Erwin, C. S. Hellberg, J. M. Sullivan, J. E. Mattson, T. F. Ambrose, A. Wilson, G. Spanos, and B. T. Jonker, Science **295**, 651 (2002).
[5] Y. Shuto, M. Tanaka, and S. Sugahara, J. Appl. Phys. **99**, 08D516 (2006).
[6] Y. X. Chen, S. S. Yan, Y. Fang, Y. F. Tian, S. Q. Xiao, G. L. Liu, Y. H. Liu, and L. M. Mei, Appl. Phys. Lett. **90**, 052508 (2007).
[7] S. Yada, S. Sugahara, and M. Tanaka, Appl. Phys. Lett. **93**, 193108 (2008).
[8] R. R. Gareev, Y. V. Bugoslavsky, R. Schreiber, A. Paul, M. Sperl, and M. Döppe, Appl. Phys. Lett. **88**, 222508 (2006).
[9] F. Tsui, L. He, L. Ma, A. Tkachuk, Y. S. Chu, K. Nakajima, and T. Chikyow, Phys. Rev. Lett. **91**, 177203 (2003).

[10]S. Cho, S. Choi, S. C. Hong, Y. Kim, J. B. Ketterson, B.-J. Kim, Y. C. Kim, and J. H. Jung, Phys. Rev. B **66**, 033303 (2002).
[11]S. Choi, S. C. Hong, S. Cho, Y. Kim, J. B. Ketterson, C. Jung, K. Rhie, B. J. Kim, and Y. C. Kim, J. Appl. Phys. **93**, 7670 (2003).
[12]R. Goswami, G. Kioseoglou, A. T. Hanbicki, O. M. J. van't Erve, B. T. Jonker, and G. Spanos, Appl. Phys. Lett. **86**, 032509 (2005).
[13]M. Jamet, A. Barski, T. Devillers, V. Poydenot, R. Dujardin, P. Bayle-Guillemaud, J. Rothman, E. Bellet-Amalric, A. Marty, J. Cibert, R. Mattana, and S. Tatarenko, Nat. Mater. **5**, 653 (2006).
[14]H. Weng and J. Dong, Phys. Rev. B **71**, 035201 (2005).
[15]A. Paul and B. Sanyal, Phys. Rev. B **79**, 214438 (2009).
[16]J. H. Yao, S. C. Li, M. D. Lan, and T. S. Chin, Appl. Phys. Lett. **94**, 072507 (2009).
[17]Y. Fukuma, H. Asada, S. Miyawaki, T. Koyanagi, S. Senba, K. Goto, and H. Sato, Appl. Phys. Lett. **93**, 252505 (2008).
[18]J. C. A. Huang, H. S. Hsu, Y. M. Hu, C. H. Lee, Y. H. Huang, and M. Z. Lin, Appl. Phys. Lett. **85**, 3815 (2004).
[19]S. J. Potashnik, K. C. Ku, R. Mahendiran, S. H. Chun, R. F. Wang, N. Samarth, and P. Schiffer, Phys. Rev. B **66**, 012408 (2002).
[20]A. Franco1, V. S. Zapf, V. B. Barbeta, and R. F. Jardim, J. Appl. Phys. **107**, 073904 (2010).
[21]S. Gangopadhyay, G. C. Hadjipanayis, B. Dale, C. M. Sorensen, K. J. Klabunde, V. Papaefthymiou, and A. Kostikas, Phys. Rev. B **45**, 9778 (1992).
[22]F. Hellman, M. Q. Tran, A. E. Gebala, E. M. Wilcox, and R. C. Dynes, Phys. Rev. Lett. **77**, 4652 (1996).
[23]W. Teizer, F. Hellman, and R. C. Dynes, Solid State Commun. **114**, 81 (2000).
[24]L. Zeng, J. X. Cao, E. Helgren, J. Karel, E. Arenholz, L. Ouyang, D. J. Smith, R. Q. Wu, and F. Hellman, Phys. Rev. B **82**, 165202 (2010).
[25]Y. Fukuma, M. Arifuku, H. Asada, and T. Koyanagi, J. Appl. Phys. **91**, 7502 (2002).
[26]A. P. Li, J. F. Wendelken, J. Shen, L. C. Feldman, J. R. Thompson, and H. H. Weitering, Phys. Rev. B **72**, 195205 (2005).
[27]C. Kittel, Phys. Rev. **110**, 1295 (1958).